

Fully parallel algorithm for simulating dispersion-managed wavelength-division-multiplexed optical fiber systems *

P. M. Lushnikov^{1,2}

¹ *Theoretical Division, Los Alamos National Laboratory, MS-B284, Los Alamos, New Mexico, 87545*

² *Landau Institute for Theoretical Physics, Kosygin St. 2, Moscow, 117334, Russia*

An efficient numerical algorithm is presented for massively parallel simulations of dispersion-managed wavelength-division-multiplexed optical fiber systems. The algorithm is based on a weak nonlinearity approximation and independent parallel calculations of fast Fourier transforms on multiple CPUs. The algorithm allows one to implement numerical simulations $M/2$ times faster than a direct numerical simulation by a split-step method, where M is a number of CPUs in parallel network.

OCIS codes: 060.2330, 060.5530, 060.4370, 190.5530, 260.2030.

A wavelength-division-multiplexed (WDM) dispersion-managed (DM) optical fiber system is the focus of current research in high-bit-rate optical communications. High capacity of optical transmission is achieved using both wavelength multiplexing and dispersion management. (See e.g. Ref.^{1,2}). Wavelength multiplexing allows the simultaneous transmission of several information channels, modulated at different wavelengths, through the same optical fiber. A dispersion-managed³⁻⁶ optical fiber systems are designed to achieve low (or even zero) path-averaged group-velocity dispersion (GVD) by periodically alternating the sign of the dispersion along an optical fiber. This dramatically reduces pulse broadening. Second-order GVD (dispersion slope) effects and path-averaged GVD effects cause optical pulses in distinct WDM channels to move with different group velocities. Consequently modeling of WDM systems requires simulating a long time interval. Enormous computation resources are necessary to capture accurately the nonlinear interactions between channels which deteriorates bit-rate capacity. The large computational resources required to simulate WDM transmission over transoceanic distances make parallel computation necessary. Here an efficient numerical algorithm is developed for massive parallel computation of WDM systems. The required computational time is inversely proportional to the number of parallel processors used. This makes feasible a full scale numerical simulation of WDM systems on a workstation cluster with a few hundred processors.

Neglecting polarization effects and stimulated Raman scattering and Brillouin scattering, the propagation of WDM optical pulses in a DM fiber is described by a scalar nonlinear Schrödinger equation (NLS):

$$\begin{aligned} & iA_z - \frac{1}{2}\beta_2(z)A_{tt} - \frac{i}{6}\beta_3(z)A_{ttt} + \sigma(z)|A|^2u \\ &= i\left(-\gamma + [\exp(z_a\gamma) - 1]\sum_{k=1}^N\delta(z - z_k)\right)A \\ & \equiv iG(z)A, \end{aligned} \tag{1}$$

where z is the propagation distance along an optical fiber, $A(t, z)$ is the slow amplitude of light; β_2 and β_3 are the first and second-order GVD respectively which are periodic functions of z ; $\sigma = (2\pi n_2)/(\lambda_0 A_{eff})$ is the nonlinear coefficient; n_2 is the nonlinear refractive index; $\lambda_0 = 1.55\mu m$ is the carrier wavelength; A_{eff} is the effective fiber area; $z_k = kz_a$ ($k = 1, \dots, N$) are amplifier locations; z_a is the amplifier spacing; and γ is the loss coefficient. Note that distributed amplification can be also included in $G(z)$ without changing the following analysis.

The change of variables $u = Ae^{-\int_0^z G(z')dz'}$ results in the NLS with the z -dependent nonlinear coefficient $c(z) \equiv \sigma(z) \exp\left(2\int_0^z G(z')dz'\right)$:

$$iu_z - \frac{1}{2}\beta_2(z)u_{tt} - \frac{i}{6}\beta_3(z)u_{ttt} + c(z)|u|^2u = 0. \tag{2}$$

*Accepted to Optics Letters (2001)

By applying Fourier transform $\hat{u}(\omega, z) = \int_{-\infty}^{\infty} u(t, z)e^{i\omega t}dt$ to Eq. (2), changing variables $\hat{u}(\omega, z) \equiv \hat{\psi}(\omega, z) \exp\left(\frac{i}{2} \int_0^z dz' [\omega^2 \beta_2(z') + \frac{\omega^3}{3} \beta_3(z')]\right)$ and integrating Eq. (2) over z from z_0 to z one obtains the following integro-differential equation:

$$\begin{aligned} \hat{\psi}(\omega, z) &= \hat{\psi}(\omega, z_0) + \\ & iR(\hat{\psi}[\omega, z], \omega, z, z_0), \end{aligned} \quad (3)$$

where

$$\begin{aligned} R(\hat{v}[\omega, z], \omega, z, z_0) &= \frac{1}{(2\pi)^2} \int d\omega_1 d\omega_2 d\omega_3 \int_{z_0}^z dz' \\ & \times c(z') \hat{v}^{(z')}(\omega_1, z') \hat{v}^{(z')}(\omega_2, z') \hat{v}^{*(z')}(\omega_3, z') \\ & \times \exp\left(-\frac{i}{2} \int_0^{z'} dz'' [\omega^2 \beta_2(z'') + \frac{\omega^3}{3} \beta_3(z'')]\right) \\ & \times \delta(\omega_1 + \omega_2 - \omega - \omega_3), \\ & \hat{v}^{(z)}(\omega, z) \equiv \hat{v}(\omega, z) \\ & \times \exp\left(\frac{i}{2} \int_0^z dz' [\omega^2 \beta_2(z') + \frac{\omega^3}{3} \beta_3(z')]\right). \end{aligned} \quad (4)$$

If the nonlinearity is small: $z_{nl} \gg z_{disp}$, where $z_{nl} \equiv 1/|p|^2$ is a characteristic nonlinear length, $z_{disp} \equiv \tau^2/|\beta_2|$ is the dispersion length; p and τ are typical pulse amplitude and width respectively. Then one can conclude that $\hat{\psi}(\omega, z)$ is a slow function of z on any scale $L \ll z_{nl}$ because all of the fast dependence of \hat{u} is already included in the term $\exp\left(\frac{i}{2} \int_0^z dz' [\omega^2 \beta_2(z') + \frac{\omega^3}{3} \beta_3(z')]\right)$ (see reference⁷⁻⁹). This term is nothing more than an exact solution of the linear part of Eq. (2). In first approximation one can neglect the slow dependence of $\hat{\psi}$ on z in the interval $mL \leq z < (m+1)L$, i.e. one can replace $\hat{\psi}[\omega, z]$ by $\hat{\psi}[\omega, mL]$ in the nonlinear term R (m is an arbitrary nonnegative integer number). This substitution allows to rewrite Eq. (3) in the following form:

$$\begin{aligned} \hat{\psi}(\omega, (m+1)L) &= \hat{\psi}(\omega, mL) + \\ & iR(\hat{\psi}[\omega, mL], \omega, (m+1)L, mL) + O\left(\frac{L}{z_{nl}}\right)^2. \end{aligned} \quad (5)$$

The term $O(L/z_{nl})^2$ indicates the order of accuracy of this approximation. Eq. (5) enables one to find $\hat{\psi}(\omega, (m+1)L)$ given $\hat{\psi}(\omega, mL)$. Thus one can recover $u(t, z)$ using the definition of ψ . However for WDM simulation, the accuracy $O(L/z_{nl})^2$ is not always sufficient. The next order approximation is obtained by including the first order correction, $\hat{\psi}^{(1)}(\omega, mL)$, in the nonlinear term, R :

$$\begin{aligned} \hat{\psi}(\omega, (m+1)L) &= \hat{\psi}(\omega, mL) \\ & + iR(\hat{\psi}^{(1)}[\omega, z], \omega, z, mL) + O\left(\frac{L}{z_{nl}}\right)^3, \end{aligned} \quad (6)$$

$$\hat{\psi}^{(1)}(\omega, z) \equiv \hat{\psi}(\omega, mL) + iR(\hat{\psi}[\omega, mL], \omega, z, mL). \quad (7)$$

Equations (4), (6), and (7) form a closed set for the approximate calculation of $\hat{\psi}(\omega, (m+1)L)$ given $\hat{\psi}(\omega, mL)$, where $O\left(\frac{L}{z_{nl}}\right)^3$ is the accuracy of the approximate solution which is controlled by the appropriate choice of L . The main obstacle in the numerical integration of Eqs. (4), (6), and (7) is the computation of the integral term $R(\hat{v}[\omega, z], \omega, z, mL)$ which generally requires $M \times N^3$ operations for each iteration, where N is the number of grid points in ω or t -space and M is the number of grid points for integration over z . Next one presents a very efficient numerical algorithm for calculations $R(\hat{v}[\omega, z], \omega, z, mL)$.

In t -space Eq. (4) becomes

$$\begin{aligned}
& \hat{F}^{-1}\left(R(\hat{v}[\omega], \omega, z, mL)\right) \\
&= \int_{mL}^z dz' c(z') \mathbf{G}^{(z')} (V^{(z')}(t, z')), \tag{8}
\end{aligned}$$

where \hat{F}^{-1} is the inverse Fourier transform over ω ; $V^{(z)}(t, z) \equiv |v^{(z)}(t, z)|^2 v^{(z)}(t, z)$ and $\mathbf{G}^{(z)}$ is the integral operator corresponding to the multiplication operator $\hat{\mathbf{G}}^{(z)}(\hat{\Psi}^{(z)}(\omega, z)) \equiv \exp\left(-\frac{i}{2} \int_0^z dz' [\omega^2 \beta_2(z') + \frac{\omega^3}{3} \beta_3(z')]\right) \hat{V}^{(z)}(\omega, z)$ in the ω -space. It follows from Eqs. (4), (6) – (8) that the numerical procedure for calculation of $R(\hat{A}, \omega)$ requires the following eight steps:

- (i) The Inverse Fourier Transform of $\hat{v}^{(z)}(\omega, mL) = \hat{\psi}(\omega, mL) \exp\left(\frac{i}{2} \int_0^z dz' [\omega^2 \beta_2(z') + \frac{\omega^3}{3} \beta_3(z')]\right)$ for every value of z ($mL < z \leq (m+1)L$).
- (ii) A calculation of $V^{(z)}(t, mL)$ from $v^{(z)}(t, mL)$.
- (iii) The Forward Fourier Transform of $V^{(z)}(t, mL)$.
- (iv) A numerical integration (summation) of $c(z') \exp\left(-\frac{i}{2} \int_0^z dz' [\omega^2 \beta_2(z') + \frac{\omega^3}{3} \beta_3(z')]\right) \hat{V}^{(z')}(\omega)$ over z' (from $z' = mL$ to $z' = z$) for every values of ω and z ($mL < z \leq (m+1)L$). This integration gives $\hat{\psi}^{(1)}(\omega, z)$ according to Eq. (7).
- (v) The Inverse Fourier Transform of $\hat{v}^{(z)}(\omega, z) = \hat{\psi}^{(1)}(\omega, z) \exp\left(\frac{i}{2} \int_0^z dz' [\omega^2 \beta_2(z') + \frac{\omega^3}{3} \beta_3(z')]\right)$ for every value of z , $mL < z \leq (m+1)L$. (Note that in contrast with step (i) it is necessary to take into account the dependence of $\hat{\psi}^{(1)}$ on z).
- (vi)-(viii) These steps are similar to steps (ii)-(iv) except that the new value of $\hat{v}^{(z)}(\omega, z)$ is used which was obtained in step (v).

The forward and inverse Fourier transforms can be performed with the fast Fourier transform (FFT) which requires $N \text{Log}_2(N)$ numerical operations. Steps (i)-(iii) need only the value of $\psi(t, mL)$. These steps can be performed independently and simultaneously in a network of M central processor units (CPUs), shown schematically in Fig. 1. The number of CPUs, M , coincides with the number of grid points for integration over z . Thus the effective computational time equals to time necessary to perform $2N \text{Log}_2(N)$ operations on complex numbers in one CPU. Below to estimate effective computational time one always refers to the number of numerical operations in one CPU if all calculations can be implemented simultaneously in different CPUs without communication between them.

The resulting values of $V^{(z)}(t, mL)$ (after step (iii)) are a set of M vectors \mathbf{a}_m , ($m = 1, 2, \dots, M$) consisting of N complex numbers each. Every vector \mathbf{a}_m is stored in the memory of the m th CPU (or in memory assigned to m th CPU in shared memory network). To perform step (iv) one replaces these vectors by the new vectors \mathbf{b}_m : $\mathbf{b}_m = \sum_{j=1}^m \mathbf{a}_j$, ($m = 1, 2, \dots, M$). Here a simple parallel algorithm is given. Note that this algorithm can be improved but this improvement is outside the scope of this Letter. It is assumed that M is a power of 2: $M \equiv 2^{M_e}$, M_e is an integer. The proposed algorithm requires M_e substeps. The vectors $\mathbf{b}_m^{(k)}$, ($m = 1, 2, \dots, M$) are results of k th substep stored in memory. So that $\mathbf{b}_m^{(M_e)} = \mathbf{b}_m$. The first substep is to sum up every pair of vectors: $\mathbf{a}_{2m} + \mathbf{a}_{2m+1}$ to get $\mathbf{b}_1^{(1)} = \mathbf{a}_1$, $\mathbf{b}_2^{(1)} = \mathbf{a}_1 + \mathbf{a}_2, \dots, \mathbf{b}_{M-1}^{(1)} = \mathbf{a}_{M-1}$, $\mathbf{b}_M^{(1)} = \mathbf{a}_{M-1} + \mathbf{a}_M$. This summation requires N operations. By induction one can see that after k substeps, $\mathbf{b}_m^{(k)} = \sum_{j=1}^m \mathbf{a}_j$ for $1 \leq m \leq 2^k$, $\mathbf{b}_m^{(k)} = \sum_{j=2^k+1}^m \mathbf{a}_j$ for $2^k + 1 \leq m \leq 2^k + 2^k, \dots, \mathbf{b}_m^{(k)} = \sum_{j=2^{M_e-2^k+1}}^m \mathbf{a}_j$ for $2^{M_e} - 2^k + 1 \leq m \leq 2^{M_e}$. Note that M vectors are now grouped in $M/2^k$ blocks with the appropriate summation inside each block. To perform the $k+1$ th substep, it is necessary to double the block size. This can be done by adding the last element of each odd block to each element of next even block. To do this, one first creates in memory of 2^k copies of the last element of each odd block, which requires kN operations in a parallel CPU network. (A number of copies can be doubled by memory forking after each N operations). To complete the $k+1$ th substep, it is now enough to simultaneously add 2^k copies to each element in the even block, requiring N operations. The total number of operations for step (iv) is $[1 + 2 + \dots + M_e]N = M_e(M_e + 1)/2$. Steps (v)-(viii) can be done in about $N[2 \text{Log}_2(N) + \text{Log}_2(M)]$ operations. (In step (viii) it is only necessary to calculate \mathbf{b}_M requiring $N \text{Log}_2[M]$ operations). Thus the total number of operation for steps (i)-(viii) is:

$$N[4 \text{Log}_2(N) + \text{Log}_2(M) + \text{Log}_2(M)]$$

$$\times (\text{Log}_2(M) + 1)/2] \sim N[4\text{Log}_2(N) + \frac{\text{Log}_2(M)^2}{2}]. \quad (9)$$

Direct solution of (2) by a split-step method with the same accuracy (for the same size of numerical step, L/M , and the same number of points N in ω space) requires $2MN\text{Log}_2(N)$ operations. Comparing this with (9), one can conclude that the proposed parallel algorithm allows one to do numerical simulations with the same numerical accuracy about $M/2$ times faster using a network of M parallel CPUs. However the proposed algorithm is about 2 times slower if only one CPU is used.

Numerical simulations of the WDM system were performed using both the split-step method for NLS (2) and using the numerical algorithm given by Eqs. (4), (6), and (7) to demonstrate the accuracy of the proposed numerical scheme. Simulations were performed for 5 WDM channels (20 Gb/s per channel) over a typical transoceanic distance of 10^4 km. The channel spacing was 0.6 nm. The GVD periodically alternates between spans of standard monomode fiber ($\beta_2^{(1)} = -20.0$ ps²/km, $\beta_3^{(1)} = 0.1$ ps³/km, $\sigma_1 = 0.0013$ (km mW)⁻¹, length $L_1 = 40$ km) and dispersion compensating fiber ($\beta_2^{(2)} = 103.9$ ps²/km, $\beta_3^{(2)} = -0.3$ ps³/km, $\sigma_2 = 0.00405$ (km mW)⁻¹, length $L_2 = -\beta_2^{(1)}L_1/\beta_2^{(2)}$ km) so that the average GVD is zero. Fiber losses and amplifiers were not considered. However they can be easily included in the coefficient $c(z)$. A pseudo-random binary sequence of length 20 was used for every WDM channel. The boundary conditions are periodic in time. Each binary “1” was represented by an initially zero-chirp Gaussian pulse (return to zero format) of 10ps width and peak power $|u|^2 = 1$ mW at the beginning ($z = 0$) of the fiber line which is taken at the middle of standard monomode fiber span. The integration length L (see Eqs. (4), (6), (7)) is set to be equal to $(L_1 + L_2)/4$; $M = 2^9$; and $N = 2^{11}$. Fig. 2 shows the pulse power distribution (simultaneously in all 5 channels) after propagating 10^4 km obtained from both the split-step and the proposed parallel algorithm. The differences in power distribution between these two simulations are less than 1% so the two curves are indistinguishable in Fig. 2. Numerical simulations were performed on usual workstation without use of parallel computations. The objective of this numerical example is to demonstrate the relative accuracy of numerical algorithm. Hardware implementation of the parallel simulation for numerical algorithm (4), (6), and (7) is beyond the scope of this Letter.

One can conclude that the proposed parallel numerical algorithm allows one to implement numerical simulations of Eq. (1) about $M/2$ times faster than a direct numerical simulation of that Eq. by the split-step method with the same accuracy. The absence of communications between parallel CPUs during the computation of the FFT allows one to implement the proposed massive parallel algorithm on workstation clusters.

The author thanks M. Chertkov, I.R. Gabitov and S. Tretiak for helpful discussions.

Support was provided by the Department of Energy, under contract W-7405-ENG-36.

E-mail address: lushnikov@crls.lanl.gov.

1. D. LeGuen, S. Del Burgo, L. Moulinard, D. Grot, M. Henry, F. Favre, T. Georges, OFC/IOOC'99, 21-26 Feb. 1999, San Diego, CA, USA
2. L.F. Mollenauer, P.V. Mamyshev, J. Gripp, M.J. Neubelt, N. Mamysheva, L. Gruner-Nielsen and T. Veng, Optics Letters, **25**, 704 (2000).
3. C. Lin, H. Kogelnik and L.G. Cohen, Opt. Lett., **5**, 476 (1980).
4. C. Kurtzke, IEEE Phot. Tech. Lett., **5**, 1250 (1993).
5. A.R. Chraplyvy, A.H. Gnauck, R.W. Tkach and R.M. Derosier, IEEE Phot. Tech. Lett., **5**, 1233 (1993).
6. N.J. Smith, F.M.Knox, N.J. Doran, K.J. Blow and I. Bennion, Electron. Lett., **32**, 54 (1996).
7. I.R. Gabitov and S.K. Turitsyn, Opt. Lett., **21**, 327 (1996).
8. I. Gabitov and S.K. Turitsyn, JETP Lett., **63**, 861 (1996).
9. P.M. Lushnikov, Opt. Lett. **26**, 1535 (2001).

Figure captions:

Fig.1. A schematic of parallel computation algorithm and required number of numerical steps. FFT_1, FFT_2, \dots represent FFT in first, second etc. CPUs respectively. Right-hand-side schematically shows calculation of vectors \mathbf{b}_m (see text).

Fig.2. Power distributions of 5 WDM channels after propagation of pseudorandom sequences of Gaussian pulses over 10^4 km. Only small part of the total computational interval of $1000ps$ is shown.

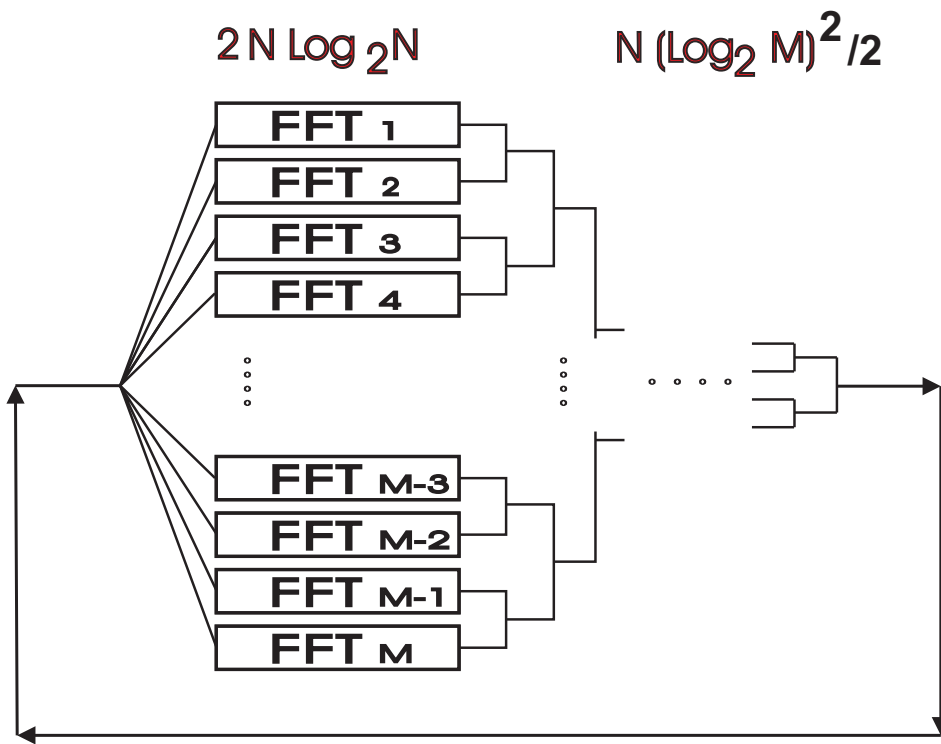


Figure 1

P. M. Lushnikov. "Fully parallel algorithm for simulating ..."
 Accepted to Optics Letters

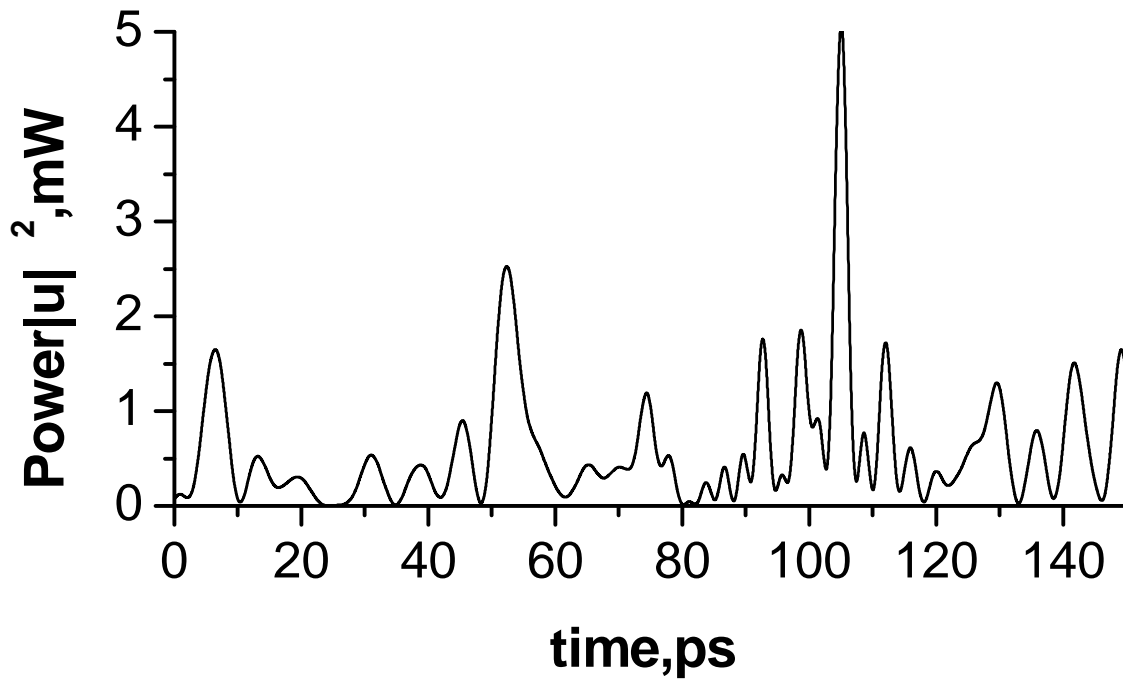


Figure2.
P.M.Lushnikov"Fullyparallelalgorithmforsimulating..."
SubmittedtoOpticsLetters